Generalized Methodology for the Analysis and Design of Multiphase Converters with Integrated Magnetics

L. Laguna, R. Prieto, O. Garcia, R. Gutierrez, J. A. Cobos
Centro de Electrónica Industrial (CEI)
Escuela Técnica Superior de Ingenieros Industriales
Universidad Politécnica de Madrid
José Gutierrez Abascal 2, Madrid, Spain
Tel.: +34 913363191 Fax: +34915645966

***Abstract*—This paper presents a methodology that can be automatized in order to analyze and design multiphase converters with coupled inductors regardless of the magnetic structure. The general procedure is to obtain a symbolic model of the converter in a generic state-space form. With this model, the expressions for the main design issues are obtained involving the magnetic and electric parameters of the converter. The validation of the procedure is presented contrasting the results with real converter measurements.**

I. Introduction

The multiphase buck converters with coupled inductors presents a number of advantages like significant improvements in the dynamic response, phase current ripple reduction, power distribution and component size reduction [1][2][3].

Different approaches of coupling on the magnetic component have been analyzed in [2], the performance of the magnetic component has been presented in [1] and an actual validation of this concept can be found in [3].

This paper presents a general methodology for the study of multiphase coupled converters that is independent of the construction of the magnetic component. The approach is to obtain a symbolic magnetic-electric state-space model of the multiphase converter and its magnetic structure using a Computer Algebra Software (CAS) like Maple or Mathematica. Once having this state-space model in matrix form, an automatic procedure can be performed to obtain the expressions in order to design the converter.

In the section II it is presented the model of the magnetic winding used to model the electric part in conjunction with the magnetic part of the converter. Also it is presented how to obtain the expressions that relate the magnetic parameters with the actual measurements of a real component. Section III presents the procedure used to obtain the state-space model of the converter. In section IV it is shown the procedure to determine the current ripple in each phase using the state-space model. Section V analyzes the dynamic response of the converter. And finally in section VI it is presented the validation of the proposed methodology comparing the results with two real converters.

II. Model of the Magnetic Component

The main goal of the magnetic component modeling approach is to obtain a symbolic (analytical) and simplified (few parameters) model that preserves the nature of the structure with a good level of accuracy.

The model of the converter analyzed in this work merges the electrical and magnetic parts of the circuit. For this purpose the following model of a winding is used (eqs. 1 and 2):

$$V = -n \cdot f' + Rl \cdot i \tag{1}$$

$$E' = n \cdot \frac{d}{dt} \cdot i \tag{2}$$

where:

$$E' = \frac{d}{dt} \cdot E \tag{3}$$

$$f' = \frac{d}{dt} \cdot flux \tag{4}$$

The graphic representation of the winding model it is shown in figure 1, it can be seen that i represents the electric current that flows through the terminals an V the voltage across terminal. On the other side, E' represents the derivative of the magnetomotive (eq. 3) force and f' represents the derivative of the flux (eq. 4). Equations 3 and 4 are used to transform the model in order to keep the electric current as a state variable in the models. The term Rl represents the resistance of the winding, and n the number of turns.

The approach is to establish a model depending on the structure of the component, for example a three phase

978-1-4244-1668-4/08/$25.00 ©2008 IEEE

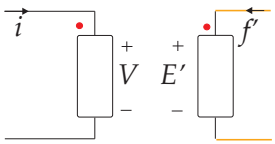

Fig. 1. Graphical representation of the winding model

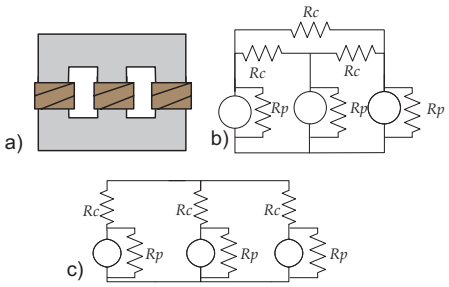

Fig. 2. Three phase magnetic component with ladder structure and its approximated models. a) component. b) symmetric model. c) non symmetric model

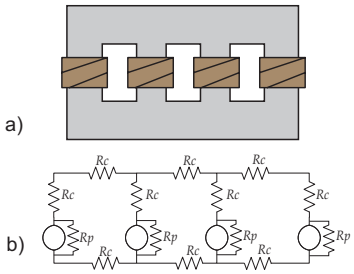

Fig. 3. Four phase magnetic component with ladder structure. a) component. b) approximated model

converter with ladder structure core (figure 2.a) can be approximated with one of the two-parameter models of figures 2.b and 2.c.

The model of any magnetic structure with any number of phases can be obtained using the same approach. The number of parameters needed depends on the complexity of the magnetic structure but the objective is to keep it as low as possible in order to simplify the expressions without affecting significantly the accuracy of the model.

Another example of a two-parameter approximated model of a four phase magnetic structure is shown in figure 3.

A symbolic analysis package for Maple was developed by the authors. This package has follow the same principle as the package presented in [4] but adds some new features in order to give more flexibility to the models. Using this package, the magnetic component is analyzed. The model shown in figure 4 is used to analyze the three-phase magnetic component. It can be seen that the model is constituted by three winding models. In the magnetic side, the leakage is represented by

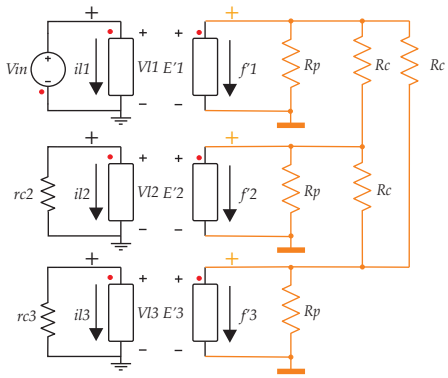

Fig. 4. Analyzed model of the three phase magnetic component (symmetric model)

the reluctances Rp, and the core paths are represented by the reluctances Rc. The winding number 1, in the electric part, has an stimulus source Vin connected. The other two windings have a resistance connected ($rc2$, $rc3$). Using the symbolic analysis program the state-space representation of this model is obtained. In order to symbolically calculate the leakage inductance (L_{leak}) and magnetizing inductance (L_{mag}) of this component the following steps are performed. First, to calculate L_{leak} and L_{mag}, make the winding resistance value negligible ($Rl \rightarrow 0$). Second, the open-circuit and short circuit conditions must be mathematically calculated. To obtain the leakage inductance (short-circuit) the resistances $rc3$ and $rc3$ are set to zero ($rc2 \rightarrow 0$, $rc3 \rightarrow 0$). And to obtain the magnetizing inductance the resistances are set to infinity ($rc2 \rightarrow \infty$, $rc3 \rightarrow \infty$). Solving the system for both cases and using the equation of the inductor (eq. 5) it is possible to obtain the relation of the magnetic parameters (Rp and Rc) with the leakage and magnetizing inductance (eqs. 6 and 7).

$$V = L \cdot \frac{d}{dt} \cdot i \tag{5}$$

$$L_{mag} = \frac{(Rc + 2 \cdot Rp) \cdot n^2}{Rp \cdot Rc} \tag{6}$$

$$L_{leak} = \frac{(Rc + 3 \cdot Rp) \cdot n^2}{Rp \cdot (Rp + Rc)} \tag{7}$$

A comparison of the model against a real three phase component is shown in figure 5. The real component was constructed using two E30/15/7 cores with windings in each leg.

The same procedure can be performed with any other magnetic structure, and this procedure can be easily automatized to obtain the needed relationships according to the number of magnetic parameters.

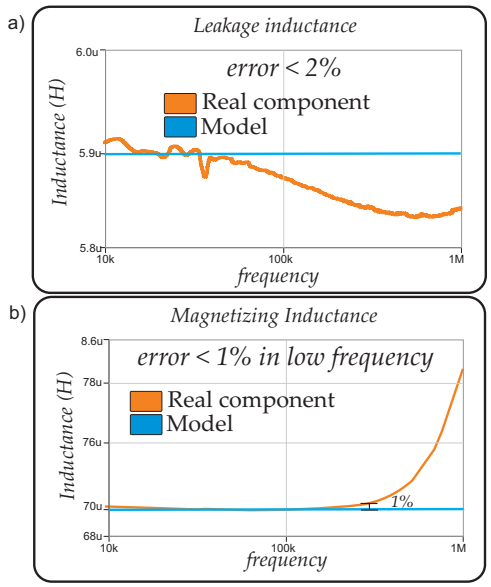

Fig. 5. Comparison between the approximated model and a real three phase component for the leakage and magnetizing inductance

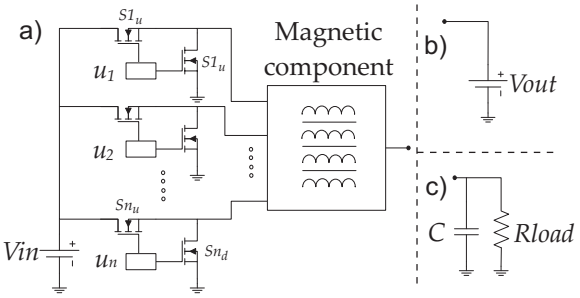

Fig. 6. Analyzed model of the converter. a) switches and magnetic component. b) output used for ripple analysis. c) output used for dynamic response analysis

III. Model of the Complete Converter

In order to perform the required analysis, two state space models of the converter were developed, each one is used in different analysis. To analyze the dynamic response of the converter, the used model is shown in figure 6.a and the model of output used is shown in 6.c, this output takes into account that the converter has a capacitor and a load resistance at the output. This model will be referred as "dynamic" model. The other model (figure 6.a with 6.b as output) is used to analyze the current ripple in each phase of the converter, this model assumes that the output capacitor is large enough and has reached the steady-state condition, this model will be referred as "ripple" model.

The state-space models are obtained performing symbolic analysis using the previously mentioned package.

The "ripple" model of any multiphase converter with coupled inductors can be represented in matrix as shown in equation 8. It can be seen in the matrix representation that the vector $\mathbf{X}$ contains the term of the current in each phase. Vector $\mathbf{u}$ contains the control signals of each phase. Matrix $\mathbf{A}$ represents the relation among the phase currents. Matrix $\mathbf{B}$ represents the effect that turning-on a phase has over the other phases. Vector $\mathbf{K}$ represents the effect of the output voltage over the phases.

$$\hat{\mathbf{X}} = \mathbf{A}\cdot\mathbf{X} + \mathbf{B}\cdot\mathbf{u} + \mathbf{K}$$

$$\mathbf{A} = \begin{bmatrix} a_{1,1} & a_{1,2} & \cdots & a_{1,N} \\ a_{2,1} & a_{2,2} & \cdots & a_{2,N} \\ \vdots & \vdots & \ddots & \vdots \\ a_{N,1} & a_{N,2} & \cdots & a_{N,N} \end{bmatrix} \quad \mathbf{X} = \begin{bmatrix} il_1 \\ il_2 \\ \vdots \\ il_N \end{bmatrix}$$

$$\mathbf{B} = \begin{bmatrix} b_{1,1} & b_{1,2} & \cdots & b_{1,N} \\ b_{2,1} & b_{2,2} & \cdots & b_{2,N} \\ \vdots & \vdots & \ddots & \vdots \\ b_{N,1} & b_{N,2} & \cdots & b_{N,N} \end{bmatrix} \quad \mathbf{u} = \begin{bmatrix} u_1 \\ u_2 \\ \vdots \\ u_N \end{bmatrix} \tag{8}$$

$$\mathbf{K} = \begin{bmatrix} k_1 \\ k_2 \\ \vdots \\ k_N \end{bmatrix} \quad \hat{\mathbf{X}} = \begin{bmatrix} i\hat{l}_1 \\ i\hat{l}_2 \\ \vdots \\ i\hat{l}_N \end{bmatrix}$$

The matrices $\mathbf{A}$ and $\mathbf{B}$ of the three phase converter with the magnetic component in figure 4 can be characterized as shown in equation 9.

$$a_{i,j}\begin{cases} \frac{-(Rc+Rp)\cdot Rp\cdot Rl}{(Rc+3\cdot Rp)\cdot n^2} & if\ i=j \\ \frac{-Rp^2\cdot Rl}{(Rc+3\cdot Rp)\cdot n^2} & if\ i\neq j \end{cases}$$

$$b_{i,j}\begin{cases} \frac{Rp\cdot(Rc+Rp)\cdot Vin}{(Rc+3\cdot Rp)\cdot n^2} & if\ i=j \\ \frac{Rp^2\cdot Vin}{(Rc+3\cdot Rp)\cdot n^2} & si\ i\neq j \end{cases} \tag{9}$$

$$k = -\frac{Rp}{w^2}\cdot Vout$$

In this case, it is assumed that the magnetic component is symmetric, this means that all phases have the same coupling factor, that is why the coefficients in the main diagonal are different. If all coefficients in the matrices $\mathbf{A}$ and $\mathbf{B}$ were the same the converter will have a perfect current equalization, this means that all current waveforms will be the same. This occurs because all derivatives will be also the same: $i\hat{l}_1 = i\hat{l}_2 = \cdots = i\hat{l}_n$. In any converter, it can be proved that if the core reluctance tends to zero ($Rc \rightarrow 0$), the derivatives will be equal (eq.10). This effect is ilustrated in figure 7.

$$\lim_{Rc\to 0} a_{i,j} = \lim_{Rc\to 0} a_{k,l}\ ,\ \lim_{Rc\to 0} b_{i,j} = \lim_{Rc\to 0} b_{k,l} \tag{10}$$

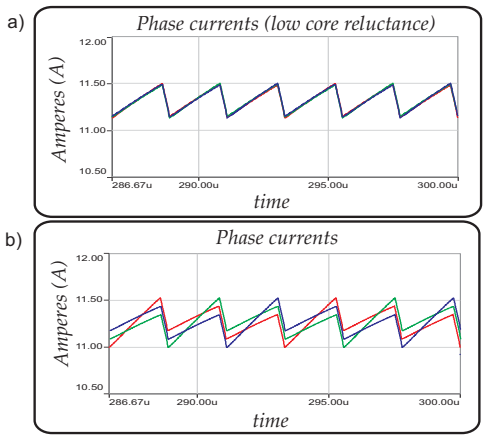

Fig. 7. Effect in the current waveforms when the core reluctance (Rc) changes. a) core with a very low reluctance. b) core with moderate low reluctance.

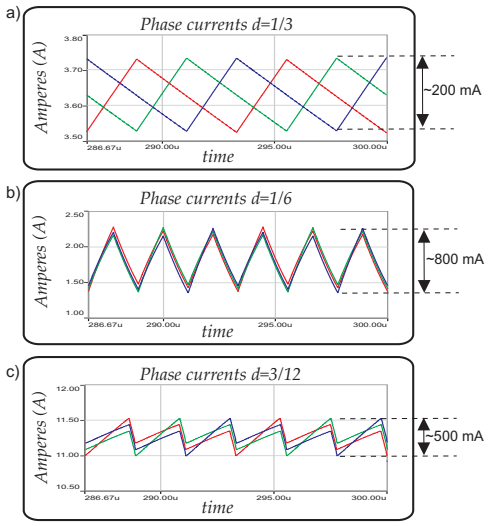

Fig. 8. Different current waveforms for the same converter (three phases) when the duty cycle changes. a) Minimum ripple point, $d = 1/3$. b) Maximum current equalization point, $d = 1/6$. c) intermediate point, $d = 3/12$.

IV. Phase Current Ripple Analysis and Operating Points of the Converter

A. Operating Points of the Converter

It is important to make a distinction between output current ripple and phase current ripple. This paper will focus on the phase current ripple because the output current ripple cancellation curve is similar to the cancellation curve in an uncoupled multiphase converter.

The observed current waveforms of one converter vary depending on the duty cycle. It is possible to define three operating points as a function of the duty cycle and the number of phases. These operating points are illustrated in figure 8. The operating point are:

- Minimum ripple point: (Figure 8.a), the main characteristic of this point is that the current waveforms have a phase shift of $360/N$ degrees (N is the number of phases), but in these points the ripple is minimum. These points occurs for any duty cycle where the number of turned-on phases is constant, e.g. in a three phase converter there are two points: $d = 1/3$ and $d = 2/3$.
- Maximum current equality point: (Figure 8.b), in this point the current wave forms tend to be very similar and it appears that there are in phase. In these points it is found the maximum current ripple. These points occurs in between the minimum ripple points. e.g. in the three phase converter the points are found in: $d = 1/6$, $d = 1/2$ and $d = 5/6$.
- Intermediate point: (Figure 8.c) for any other duty cycle the ripple is lower than the ripple found in the maximum current equalization points, and the waveforms tend to be more similar that the waveforms of the minimum ripple point.

This behavior can be easily explained if the values of the component $\mathbf{B}\cdot\mathbf{u}+\mathbf{K}$ of the state-space model are observed for different switching sequences (depending on the duty cycles). In order to group the input terms, the substitution shown equation 11 in is used.

$$\dot{\mathbf{X}} = \mathbf{A}\cdot\mathbf{X} + \mathbf{BUK}$$
$$\mathbf{BUK} = \mathbf{B}\cdot\mathbf{u} + \mathbf{K} = \begin{bmatrix} buk_1 \\ buk_2 \\ \vdots \\ buk_N \end{bmatrix} \quad (11)$$

The term buk_i represents the input of the phase i as function of the control signals in vector $\mathbf{u}$.

Two examples of the input values are shown in figure 9 for a three phase converter. Figure 9.a shows the case when the converter is working in a minimum ripple point, it can be seen that the values of the terms buk_i have a slight change. This input produces a soft change in the phase currents. Also can be seen that the buk_i terms have a clear phase shift of $360/N$ degrees. On the other case, in the maximum current equalization point (figure 9.b) it can be seen that the changes are more abrupt and the buk_i values seem to be very similar, this makes the phase currents look in phase and so alike.

B. Phase Ripple Calculation

In this section there are presented two ways to calculate the peak-to-peak current of any phase. The first one assumes that the winding resistance value is negligible, this results in an approximated expression for the peak-to-peak current. The other method takes into account the voltage drop produced by winding resistance and the phase current but uses an empirical formula, this gives a more accurate result when the winding resistance is less that 1 Ω. The objective of these

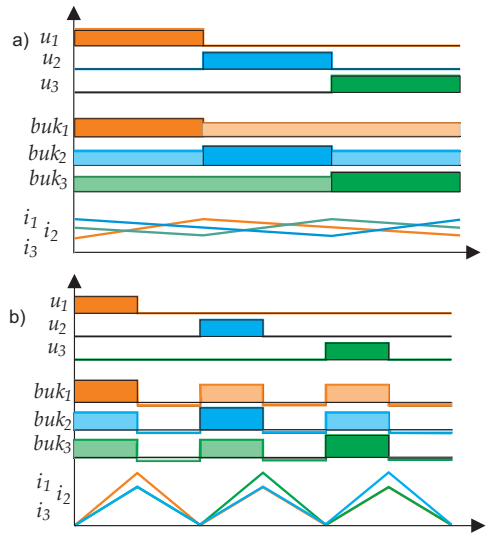

Fig. 9. Graphical explication of the converter's waveforms behavior. a) Minimum ripple point. b) Maximum current equalization point.

TABLE I
SWITCHING STATES AND TIME FOR A THREE PHASE CONVERTER WITH $d = 1/3$

State	u_1	u_2	u_3	time in this state
u1	1	0	0	$1/3 \cdot T$
u2	0	1	0	$1/3 \cdot T$
u3	0	0	1	$1/3 \cdot T$

TABLE II
SWITCHING STATES AND TIME FOR A THREE PHASE CONVERTER WITH $d < 1/3$

State	u_1	u_2	u_3	Time in this state
u1	1	0	0	d/T
u2	0	0	0	$(1/3 - d)/T$
u3	0	1	0	d/T
u4	0	0	0	$(1/3 - d)/T$
u5	0	0	1	d/T
u6	0	0	0	$(1/3 - d)/T$

two methods is to provide approximated expressions without complicate formulas.

First of all it is needed to determine the switching states and the time that lasts each state for any duty cycle. Two examples of the wanted data are presented in tables I and II for a duty cycle equal to $1/3$ and for any duty cycle less that $1/3$ respectively. A simple algorithm was written in Maple to obtain this information for any duty cycle and any number of phases.

Once having the values of the vector $\mathbf{u}$ for any switching state, when the winding resistance is small the peak-to-peak current is calculated using only the terms $\mathbf{B} \cdot \mathbf{u} + \mathbf{K}$, because

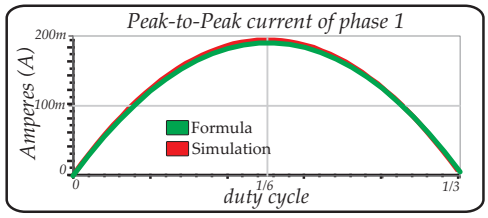

Fig. 10. Comparison between the theoretical current ripple of a three phase converter and the simulation result.

the effect of the matrix $\mathbf{A}$ is negligible. For the three phase converter the peak-to-peak current is calculated as shown in equation 12 for the first section ($0 > d > 1/3$). It is assumed that the output voltage is equal to the input voltage multiplied by the duty cycle (eq. 13).

$$\Delta \begin{bmatrix} il_1 \\ il_2 \\ il_3 \end{bmatrix} = (\mathbf{B} \cdot \mathbf{u}1 + \mathbf{K}) \cdot T/3 \tag{12}$$

$$Vout = Vin \cdot d \tag{13}$$

The formula obtained to calculate the peak-to-peak current of the phase 1 for the three phase converter is shown on equation 14, this is valid for the section were $0 > d > 1/3$. The comparison between the formula and simulation results is shown in figure 10

$$\Delta il_i = \frac{d \cdot Rp \cdot Vin \cdot (Rp - d \cdot 3 \cdot Rp - Rc \cdot d)}{f \cdot n^2 \cdot (3 \cdot Rp + Rc)} \tag{14}$$

A Maple script has been written in order to automatize this process for any section of the duty cycle and for any converter. It is only necessary to provide the matrices $\mathbf{B}$ and $\mathbf{K}$ of the converter and phase turn-on sequence (the turn-on sequence plays an important role, this will be shown in section VI).

The second method to calculate the peak-to-peak current follows almost the same approach, the main difference is that it assumes that the voltage drop due to the winding resistance (Rl) and the peak current (Δil_i) produced by the matrix $\mathbf{A}$ can be approximated introducing the substitution 15 in equation 14.

$$Vin \rightarrow Vin - \frac{\Delta il_i}{2} \cdot Rl^2 \tag{15}$$

As said before this approximation provides very good results when $Rl < 1\Omega$. A comparison of the new formula (equation 16) is shown in figure 11.

$$\Delta il_1 = \frac{((3 \cdot d - 1) \cdot Rp^2 + (d-1) \cdot Rc \cdot Rp) \cdot d \cdot Vin}{(-3 \cdot Rp - Rc) \cdot f \cdot n^2 + ((3 \cdot d - 1) \cdot Rp^2 + (d-1) \cdot Rc \cdot Rp) \cdot Rl^2} \tag{16}$$

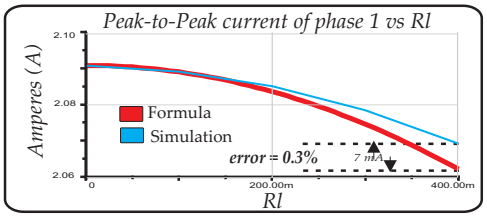

Fig. 11. Comparison between the proposed method to calculate the peak current when the Rl is significant, and the simulation results.

V. Dynamic Response vs Phase Current Ripple

Using the dynamic state-space model, the transfer function of the converter for the output voltage can be obtained by averaging methods [4]. For the three phase converter, the transfer function can be written as the transfer function of a buck converter (eq. 17) with the substitutions shown in equations 18 and 19.

$$\frac{vC(s)}{d(s)} = \frac{Rload \cdot Vin}{s^2 \cdot Leq \cdot C \cdot Rload + s \cdot Leq + Rl \cdot C \cdot Rload \cdot s + Rl + Rload} \quad (17)$$

$$Leq \rightarrow \frac{n^2}{3 \cdot Rp} \quad (18)$$

$$Rl \rightarrow \frac{Rl}{3} \quad (19)$$

As can be seen in the transfer function, the dynamic does not depend on the Rc parameter. In order to obtain the transfer function of any multiphase converter a Maple script has been written. The same analysis can be performed for any magnetic structure and the same conclusion can be drawn: *the dynamic response of the converter depends only on the leakage inductances*.

In order to improve the dynamic response, a low leakage inductance could be desired, but the analysis on the peak-to-peak current (equation 14 or 16 for the three-phase converter) shows that the ripple increases as the leakage inductance decrease. Therefore it is needed to establish a good trade off in terms of the losses of the converter in order to appropriately design the converter.

An example of a converter that takes advantage of the behavior when operating in the minimum ripple point is shown in [5], this converter has a very high dynamic response and a low phase current ripple.

VI. Experimental Results

Two magnetic components have been constructed, one for three phases (figure 12.a) and the other one for four phases (figure 12.b). Both are controlled by a board that can drive up to sixteen phases (figure 12.c) and it is controlled by an FPGA.

Figures 13 and 14 show some of the captured current waveforms of the two converters. Figure 15 presents the validation of the formula obtained for the three phase converter in the whole range of duty cycle.

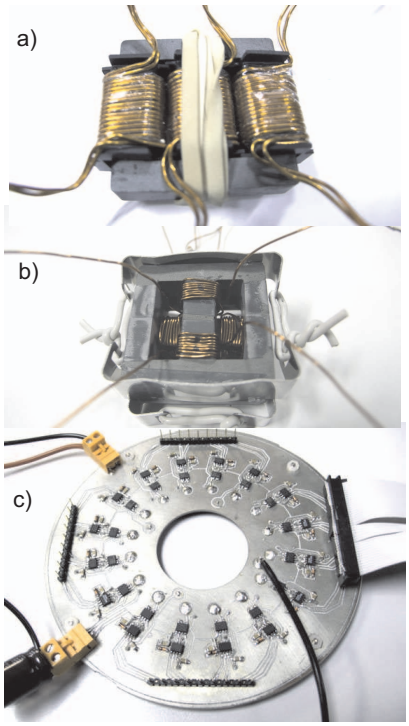

Fig. 12. Prototype converter. a) three phase magnetic component. b) four phase magnetic component. c) driving PCB

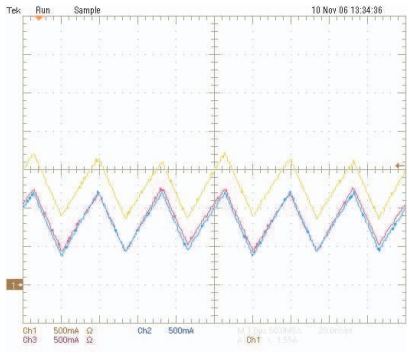

Fig. 13. Current waveforms of the three phase prototype

The four phase magnetic component (figure 12.b) was built using four pieces of E30/15/7 core and 3F3 material. It was constructed as shown in figure 16, and the model was a three-parameter symbolic model. This model assumes that the coupling between phases in the same layer is tighter than the coupling between phases in different layers. The accuracy of the symbolic model of the four phases magnetic component is as good as the model of the three phase converter (figure 5). The most interesting part of this model is that using the script to calculate the ripple presented in section IV, it is possible to define the optimal switching sequence for a

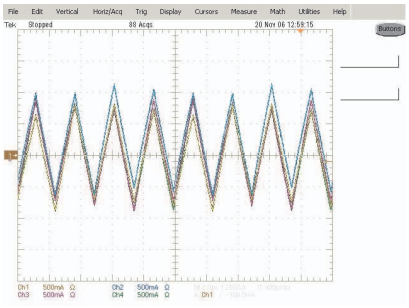

Fig. 14. Current waveforms of the four phase prototype

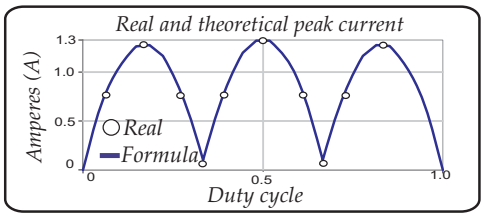

Fig. 15. Comparison of the formula of the three phase converter and the actual measurements of the real converter

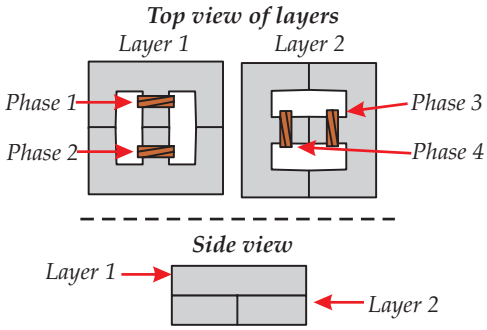

Fig. 16. Construction of the four phase magnetic component

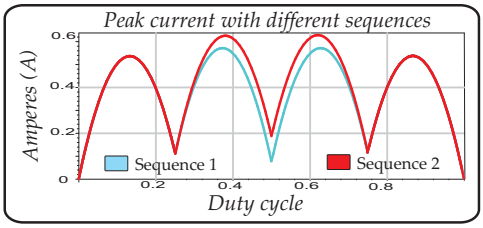

Fig. 17. Current ripple of the four phase converter with two different switching sequences

point of operation of the converter. The figure 17 presents a graphical representation of the ripple formula obtained using two different switching sequences. The first one is: $u1$,$u3$,$u2$,$u4$. This sequence turns on a phase in each layer alternated. The second sequence is: $u1$,$u2$,$u3$,$u4$. It can be seen from figure 17 that the second sequence has more ripple in the range $1/4 < d < 3/4$.

VII. Conclusions

When designing a multiphase converter, the current ripple at each phase must be taken into account in order to optimize the dynamic response and the efficiency of the converter.

A complete methodology to analyze multiphase converters with coupled inductors with any magnetic structure is presented. This methodology studies the model in symbolic way and defines procedures that can be performed automatically to provide expressions of the main issues when designing this kind of converters, like:

- dynamic response
- current equalization
- current ripple
- optimal switching sequence

Also these expressions are useful to design avoiding undesired effects like increase of current ripple due duty cycle variation, core saturation and excessive AC conduction losses.

Depending on the duty cycle (d) and the output current, it is necessary to establish the number of phases that the converter should have. This is necessary because the phase current ripple depends mainly on the duty cycle (d), the number of phases (N) and the leakage inductance. It is also recommended to design the magnetic component with a low core reluctance in order to have a high current equalization ratio.

References

[1] Jieli Li, C.R. Sullivan, and A. Schultz. Coupled-inductor design optimization for fast-response low-voltage dc-dc converters. *Applied Power Electronics Conference and Exposition, 2002. APEC 2002. Seventeenth Annual IEEE*, 2:817–823 vol.2, 2002.

[2] P. Zumel, O. Garcia, J.A. Cobos, and J. Uceda. Magnetic integration for interleaved converters. *Applied Power Electronics Conference and Exposition, 2003. APEC '03. Eighteenth Annual IEEE*, 2:1143–1149 vol.2, 9-13 Feb. 2003.

[3] Jieli Li, A. Stratakos, A. Schultz, and C.R. Sullivan. Using coupled inductors to enhance transient performance of multi-phase buck converters. *Applied Power Electronics Conference and Exposition, 2004. APEC '04. Nineteenth Annual IEEE*, 2:1289–1293 vol.2, 2004.

[4] Jian Sun and H. Grotstollen. Symbolic analysis methods for averaged modeling of switching power converters. *Power Electronics, IEEE Transactions on*, 12(3):537–546, May 1997.

[5] M.C. Gonzalez, L. Laguna, P. Alou, O. Garcia, J.A. Cobos, and H. Visairo-Cruz. New control strategy for energy conversion based on coupled magnetic structures. *Power Electronics Specialists Conference, 2008. PESC 08. 2008 IEEE 39th Annual*, 15-19 June 2008.